Influence of DNA Binding Dyes on Bare DNA Structure Studied with Atomic Force Microscopy

ARTICLE *in* MACROMOLECULES · MARCH 2015

Impact Factor: 5.8 · DOI: 10.1021/ma502537g

5 AUTHORS, INCLUDING:

Aleksandre Japaridze
École Polytechnique Fédérale de Lausanne
8 PUBLICATIONS **7** CITATIONS
SEE PROFILE

Alexander Benke
École Polytechnique Fédérale de Lausanne
10 PUBLICATIONS **88** CITATIONS
SEE PROFILE

Carine Benadiba
École Polytechnique Fédérale de Lausanne
13 PUBLICATIONS **177** CITATIONS
SEE PROFILE

Macromolecules

Article

pubs.acs.org/Macromolecules

Influence of DNA Binding Dyes on Bare DNA Structure Studied with Atomic Force Microscopy

Aleksandre Japaridze,[†] Alexander Benke,[‡] Sylvain Renevey,[†] Carine Benadiba,[†] and Giovanni Dietler*[,†]

[†]Laboratory of Physics of Living Matter and [‡]Laboratory of Experimental Biophysics, EPFL, 1015 Lausanne, Switzerland

Supporting Information

ABSTRACT: Fluorescent dyes are widely used for staining and visualization of DNA in optical microscopy based methods. Even though for some dyes the mechanism of binding is known, how this binding affects DNA remains poorly understood. Here we present a novel experimental study of the influence of staining dyes on DNA properties. We use atomic force microscopy which allows quantification and measurement of structural properties of stained DNA with nanometer resolution. We studied the influence of dyes on the persistence length, the total contour length, and the morphology of individual DNA molecules. We tested three widely used dyes known to differently bind DNA molecules, namely PicoGreen, Dapi, and DRAQ5. Based on our measurements, when imaged at typical concentrations (manufacturer suggested concentrations used for cell imaging), PicoGreen dye showed little effect, Dapi dye decreased the DNA persistence length, and DRAQ5 decreased the persistence length and elongated the DNA. When used at high concentrations, all of the dyes induced drastic changes in the DNA morphology. Our study clearly shows that DNA-binding dyes, irrespective of their DNA binding mechanisms, strongly influence the physical properties of DNA. These changes are strongly dose and dye type dependent and therefore should be taken into consideration when conducting experiments with DNA.

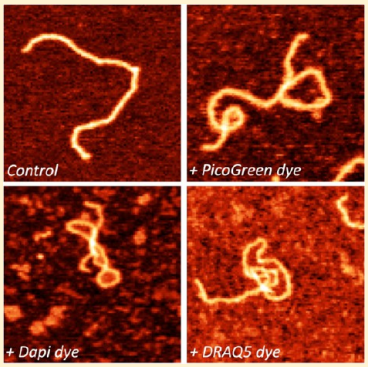

INTRODUCTION

Fluorescence microscopy is a widely used technique in cell biology, biochemistry, and medicine among other fields of scientific research. The need to label and visualize DNA and chromatin is gaining importance in different fields of biological research, with experiments ranging from measurements on isolated DNA[1−6,11−13] to experiments in fixed cells and live cells.[7−10,14]

There is a large variety of DNA labeling dyes: some binding to the minor/major grooves of double-stranded DNA, others intercalating into DNA, and some doing both.[1,8−20] The influence of DNA labeling dyes on the DNA structure and its properties is still a topic of debate, since no clear data exist on how strongly they influence physical properties.[11−19] Nevertheless, several works revealed that parameters such as the contour length and the persistence length of bare DNA can be significantly changed by fluorescent dyes upon binding.[11−20]

On the example of YOYO-1 dyes, Günther et al. showed that the intercalation of the dye in double-stranded DNA modified its mechanical and structural properties.[11] Different studies showed that upon binding of YOYO dye the contour length of the DNA increased roughly linearly, reaching 30−40% elongation compared to bare DNA. In experiments performed with optical tweezers Sischka et al. compared different DNA binding agents with different binding modes (such as ethidium bromide, YO-1, distamycin-A, and YOYO), revealing changes in the mechanical response of DNA pulling as the function of the corresponding dye binding mechanisms.[16] Wojcik et al. showed that DRAQ5 dye detached H1 and H2B histones in a concentration dependent manner in live cells.[14] Higher concentrations of the intercalator caused significant aggregation and partial loss of chromatin organization. The chromatin reorganization was proposed to happen as DRAQ5 intercalated into DNA, unwinding it and weakening the binding of the histones. In a more recent study Nyberg et al. showed that the binding of YOYO dye resulted in heterogeneous DNA staining extension. The level of resulting DNA extension depended not only on dye concentration but also on ionic strength and temperature.[21] Despite observing significant changes in the DNA morphology, detailed molecular mechanism behind those phenomena have been poorly understood.[11−21]

In our study we test how DNA binding dyes affect nanoscale DNA organization and structure. We used atomic force microscopy (AFM), a widely used technique in bio-nanosciences with nanometer spatial resolution.[22−24] AFM enabled us to directly visualize and measure physical properties of individual stained DNA molecules. We performed experiments with three widely used dyes in cell biology and biophysics that differently bind to DNA and have different emission spectra, namely PicoGreen, Dapi, and DRAQ5.

We measured the contour length and the persistence length of a linear DNA fragment labeled with different concentrations of studied dyes. Our work reveals that dyes indeed change the properties of DNA compared to its bare form.

Received: December 16, 2014
Revised: February 19, 2015
Published: March 5, 2015

DOI: 10.1021/ma502537g
Macromolecules 2015, 48, 1860−1865

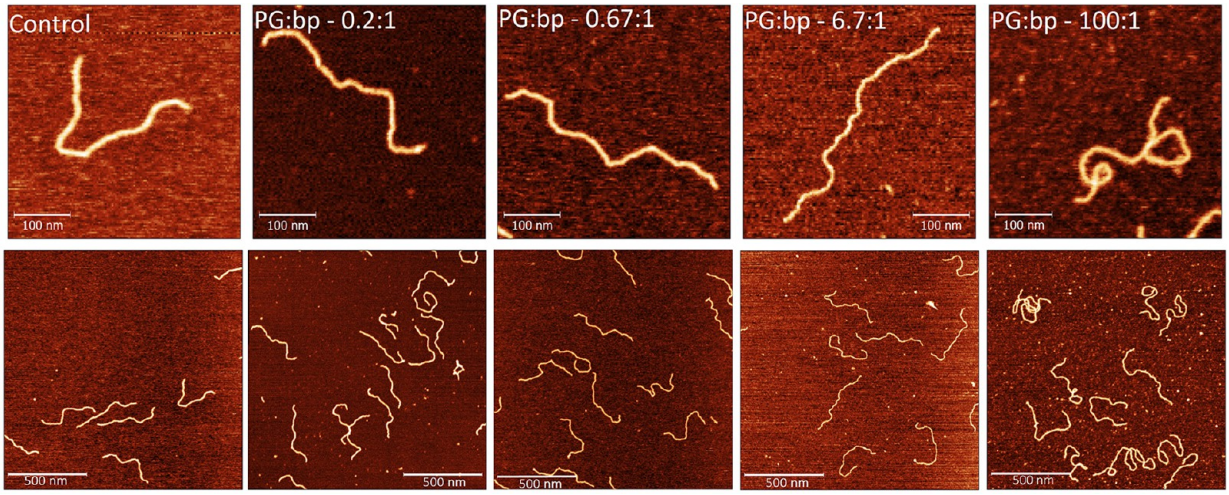

Figure 1. AFM images of control and PicoGreen stained DNA. High concentration of PicoGreen leads to more elongated DNA structures with more crossovers and finally compact structures. Scale bars for upper and lower AFM images are 100 and 500 nm, respectively.

MATERIALS AND METHODS

Linear DNA. The basis of the linear 1.4kb DNA (UPPU) was Fis (U) and H-NS (P) protein binding sites amplified from the tyrT uas sequence (primer pair: cgggatccctttgtttacggtaatcg and ccacaagcttgaactctagaacgcactctcgattcgtag) and the proV gene, respectively (primer pair: ccacaagcttgaactctagagccacatttgccatcagggg and cgggatccgccagactggcgtcttttac). UP intermediate sequences were constructed by joining U and P sequences via *Bam*HI restriction and ligation, cloned in pUC18 using *Hin*dIII and *Eco*RI restriction sites. In a second cloning step UP and PU were amplified from the intermediate UP plasmid and combined via XbaI and NheI compatible sticky end ligation, removing XbaI and NheI restriction sites and cloned in pUC18 using *Hin*dIII and *Eco*RI sites.

Linear 1.4kb fragments were further extracted from 1.5% agarose gel and purified using extraction kit from Promega. DNA was then placed in TE buffer composed of 10 mM Tris and 1 mM EDTA solution.

AFM. AFM images were collected using a MultiMode SPM with a Nanoscope III controller (Veeco Instruments, Santa Barbara, CA) operated in tapping-mode in air. The AFM cantilevers used in air had a spring constant of 5 Nm^{-1} (Veeco cantilevers, TAP150A) with resonance frequencies ranging between 120 and 160 kHz. All the recorded AFM images consist of 512 × 512 pixels with scan frequency ≤1 Hz recorded at 1.5 × 1.5 μm scale. Images were simply flattened using the Gwyddion software (Version 2.25),[25] and no further image processing was carried out.

DNA Persistence Length. The persistence length is a basic mechanical property of polymers that quantifies its conformation and flexibility. The persistence length of a DNA is defined as the typical length at which the correlation between two DNA segments decays exponentially (Supporting Information Figure S1). A typical value of L_p for double-stranded DNA is estimated to be ∼50 nm.[26−30]

We measured the persistence length L_p of DNA by directly fitting the bond correlation function for polymers in 2D (DNA is deposited on an atomically flat mica surface):

$$\langle \cos \theta(s) \rangle \sim \exp(-s/2L_p) \quad (1)$$

where θ is the angle between the tangent vectors to the chain at two points separated by the distance s and L_p the persistence length.[26−30] For samples with the highest dye concentration we used the bond correlation function in 3D (Supporting Information 1 and 2).

DNA Tracing. AFM images were analyzed using "DNA Trace", a homemade Java written analysis software. To measure the length of DNA molecules, typically 50−100 molecules were traced in the following way: first, the user manually chooses several points along a DNA molecule by simply placing the cursor on them and clicking. The tracing algorithm then calculates the shortest and, at the same time, the highest path between the two points, by solving the graph of all possible pixel pathways. Based on the statistics of 50−100 individual molecules the contour length, the end-to-end distance distribution and the bond correlation function are calculated by "DNA Trace"software.[31]

DNA Binding Dyes. Three different dyes have been used for our study: PicoGreen, DAPI, and DRAQ5.

PicoGreen dye (552.5 g/mol) (Quant-iT PicoGreen dsDNA Assay Kit purchased from Invitrogen, stock solution 0.2 mM) was used in the following dye:base pair (bp) ratios: 0.2:1; 0.67:1; 6.7:1; and 100:1. The absolute concentration of PicoGreen was determined by measuring the optical density of the solution using extinction coefficient of E_{500} = 70 000 M^{-1} cm^{-1} at room temperature similarly as described elsewhere.[12,36]

Dapi dye (457.5 g/mol) (purchased from Sigma-Aldrich, stock solution 11 mM) was used in the following dye:bp ratios: 0.33:1; 0.67:1; 6.7:1; and 50:1.

DRAQ5 dye (412.5 g/mol) (purchased from Biostatus, stock solution 5 mM) was used in the following dye:bp ratios: 0.29:1; 0.67:1; 6.7:1; and 20:1.

Typical concentrations used in staining are different for each dye and manufacturers suggest an optimal dilution factor of the stock solution, rather than the absolute concentration. In our work we qualitatively call these concentrations, typically used for staining in optical microscopy "low concentrations" (dye:bp = 0.2:1−0.67:1). The concentrations which are above this normally suggested range we qualitatively call "high concentrations" (dye:bp = 6.7:1−100:1).

AFM Buffer. All AFM samples were prepared in the AFM Buffer consisting of 1 mM Tris and 4 mM $MgCl_2$ (pH = 7.0).

Sample Preparation. A control DNA sample was first prepared by mixing the 1.4kb DNA (typical concentration of 0.5−1 ng/μL) and the AFM buffer in 20 μL volume and deposited on a freshly cleaved mica. After 5 min of deposition the mica was rinsed with 1 mL of double distilled water and dried under a gentle nitrogen flow.

For the samples containing dyes, the dyes were first diluted in the AFM buffer accordingly to the desired dye:DNA ratio (final DNA concentration of 0.5−1 ng/μL). The DNA was then added in the solution and left for 15 min for incubation at room temperature (22 °C). Afterward, the whole mix was deposited on freshly cleaved mica for 5 min before being rinsed with 1 mL of double distilled water and dried with a gentle flow of nitrogen.

Gel Electrophoresis. The gel electrophoresis experiment was performed in 1% agarose gel prepared in 1× TAE buffer. During electrophoresis the gels were submerged in 1× TAE buffer and the sample run at 50 V for 4 h. Afterward, the gel was stained using GelRed (purchased from Biotium) bath for 1 h.

DOI: 10.1021/ma502537g
Macromolecules 2015, 48, 1860−1865

RESULTS

PicoGreen. The first dye used in our experiments, PicoGreen, binds by two processes: its quinolinium group intercalates into DNA while the two dimethylaminopropyl groups lie deep in the minor groove.[7,12,20,36] The emission fluorescence spectra of PicoGreen is at ∼530 nm, and its excitation maximum is at ∼485 nm (Supporting Information 3). When bound to dsDNA, the fluorescence enhancement of PicoGreen is extremely high with very little background, with the unbound dye having almost no fluorescence. PicoGreen is very stable to photobleaching, allowing longer exposure times and assay flexibility; therefore, it is very widely used in microscopy.[7,10,12,20,36]

As the first step, we stained 1.4kb linear DNA fragment with increasing concentration of PicoGreen dye and imaged the samples with AFM. Figure 1 shows typical images of bare DNA and DNA stained with different amount of PicoGreen dye. As expected, at low PicoGreen concentration (see Materials and Methods) we did not observe any significant difference between the physical properties of control and stained DNA. The results changed once we compared bare DNA with stained DNA at high concentrations. We directly noticed a difference in DNA shape and morphology (Figure 1). DNA stained with high PicoGreen concentrations appeared to be longer in length and much more bent. On the stained samples, we observed loops and crossings that were previously absent at lower dye concentrations.

After visual comparison, the DNA fragments were traced and the histograms of contour length plotted. Figure 2 reveals a tight

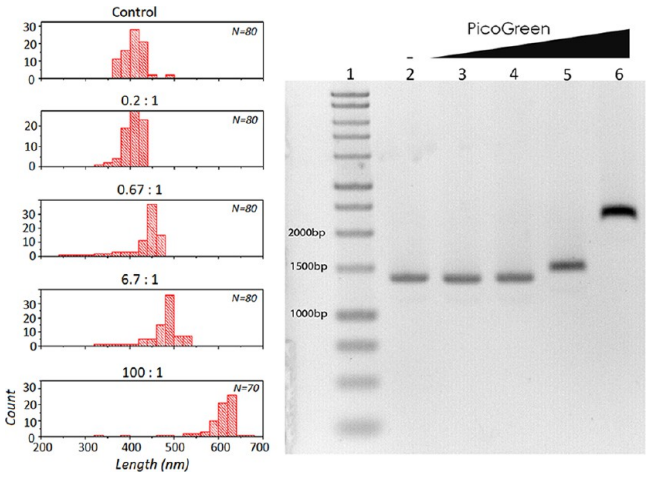

Figure 2. (A, left) Contour length distribution for DNA–PicoGreen complexes. (B, right) The corresponding DNA gel electrophoresis image. Lane 1 is the marker DNA, lane 2 control 1.4kb DNA, and lanes 3–6 show DNA stained with growing PicoGreen concentration (PicoGreen:bp = 0.2:1; 0.67:1; 6.7:1; and 100:1).

relation between DNA contour length and the PicoGreen concentration. With increasing dye concentration DNA length distribution increased progressively. Notably, the average contour length of bare DNA L ∼ 410 ± 25 nm increased by ∼45% with the highest dye concentration, reaching a value of L ∼ 600 ± 55 nm. To confirm this DNA length extension, upon PicoGreen binding, we checked the behavior of stained DNA fragments on gel electrophoresis experiment. As expected, DNA bands migrated much slower than control DNA indicated on the gel electrophoresis results (Figure 2). Surprisingly, calculating the persistence length by the bond correlation function given in eq 1 did not reveal any dependence on the staining concentration. The value stayed almost unaffected L_p ∼ 60 ± 3 nm (Supporting Information 2).

From our measurements, we could conclude that high concentrations of PicoGreen dye strongly increased the contour length of the DNA and changed the overall shape of the DNA without affecting its persistence length (Table 1).

Table 1. Shape Parameters of DNA Bound with PicoGreen Dye

PicoGreen:bp	no. of molecules	av length L [nm]	elongation [%]	L_p [nm]
control	80	410 ± 25		61 ± 3
0.2:1	80	410 ± 20		63 ± 3
0.67:1	80	430 ± 45	5	59 ± 3
6.7:1	80	480 ± 40	16	64 ± 3
100:1	70	600 ± 55	46	61 ± 3

Dapi. The second dye used in the study was Dapi. Dapi binds to the minor groove in AT base-pair-rich regions and was shown that it needs a run of 2 to 4 A′T base pairs to bind.[13,32−35,38] The emission maximum of Dapi when bound to DNA is at 460 nm, and the excitation maximum is at 358 nm (Supporting Information 3).

Similarly to the previous experiments with PicoGreen, in the case of Dapi, we imaged 1.4kb linear DNA with increasing concentration of the dye and studied its physical properties. Figure 3 shows typical images of DNA samples labeled with different Dapi concentrations. Images show that DNA gets deformed when labeled with the dye. At the highest Dapi concentration, the DNA fragments formed loops and had much more compact structure than the relaxed bare DNA (Figure 3). Compared to PicoGreen dye, Dapi did not change the average length of the DNA fragments as seen from the contour length distribution as well as the gel electrophoresis image in Figure 4. Although the contour length of DNA stayed intact, the persistence length changed strongly, decreasing proportionally with the increasing dye concentration (Table 2) (Supporting Information 2). The initial persistence length of a bare DNA fragment of L_p ∼ 60 ± 3 nm decreased and reached L_p ∼ 35 ± 3 nm for the sample with the highest Dapi concentration (∼40% decrease in the persistence length).

Based on our measurements, Dapi dye did not change the total length of the DNA but strongly influenced the morphology of it, making the structures more compact and condensed. In extreme case, the apparent persistence length of the DNA decreased by 40% compared to nonstained DNA.

DRAQ5. The last dye tested in our experiments was DRAQ5, which is known to intercalate into the double-stranded DNA as well as bind to the minor groove in AT base-pair-rich regions. Interestingly, this dye is often used for live cell imaging.[8,9,14,37] Its excitation maximum is at 646 nm and emission spectra at 697 nm.

DRAQ5 stained samples showed even stronger changes in the DNA properties compared to PicoGreen and Dapi. Figure 5 shows typical AFM images of the samples corresponding to different concentrations of dye. The morphology of the DNA as well as the total length was drastically affected by the presence of the dye. The DNA fragments became longer with increasing concentration of the dye and migrated slower in the gel electrophoresis experiment (Figure 6). Even at the highest dilution factor of 1000× DRAQ5 used in the experiment, DNA was ∼15% longer than in the control sample. The persistence

DOI: 10.1021/ma502537g
Macromolecules 2015, 48, 1860−1865

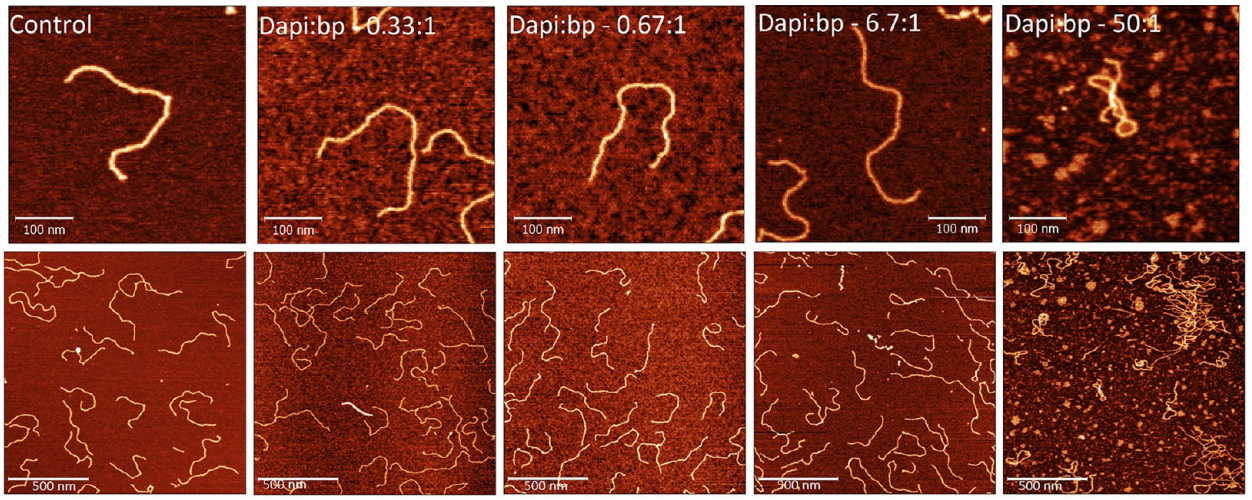

Figure 3. AFM images of control and Dapi stained DNA. High concentration of Dapi leads to more flexible and collapsed DNA structures with many crossovers. Scale bars for upper and lower AFM images are 100 and 500 nm, respectively.

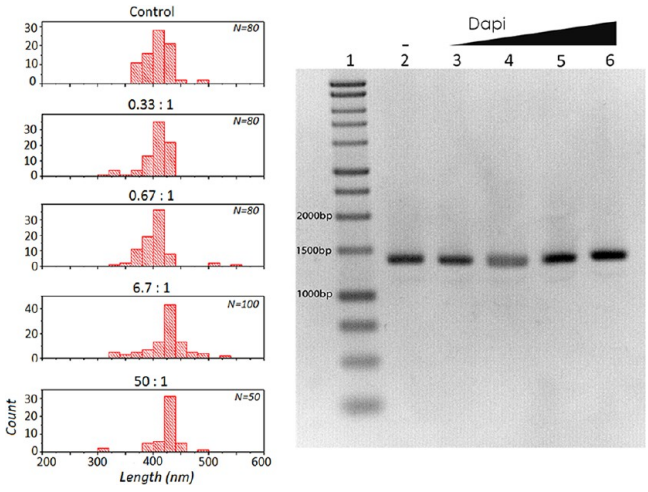

Figure 4. (A, left) Contour length distribution for DNA−Dapi complexes. (B, right) The corresponding DNA gel electrophoresis image. Lane 1 is the marker DNA, lane 2 control 1.4kb DNA, and lanes 3−6 show DNA stained with growing Dapi concentration (Dapi:bp = 0.33:1; 0.67:1; 6.7:1; and 50:1).

Table 2. Shape Parameters of DNA Bound with Dapi Dye

Dapi:bp	no. of molecules	av length L [nm]	L_p [nm]	ΔL_p [%]
control	80	410 ± 25	61 ± 3	
0.33:1	80	405 ± 25	52 ± 3	−15
0.67:1	80	400 ± 30	47 ± 3	−23
6.7:1	100	425 ± 40	42 ± 3	−31
50:1	50	420 ± 30	35 ± 3	−42

length of the DNA was also strongly modified. The initial value decreased by ∼45% and reached a value of L_p ∼ 33 ± 3 nm (Table 3) (Supporting Information 2).

On the basis of our data, we could conclude that DRAQ5 dye strongly interacted with DNA and changed the physical properties of DNA. It increased the total length of DNA fragments by ∼30% and decreased simultaneously the persistence length by ∼45%.

CONCLUSION

In this study we test how DNA binding dyes affect nanoscale organization and structure of bare DNA. Three different dyes with different binding modes were studied, with the resulting data giving us the possibility to compare these three dyes among each other.

We compared the dye concentration at which significant structural changes in the DNA−dye complexes started to appear. Surprisingly even at low concentrations, both Dapi and DRAQ5 strongly influenced the morphology of the DNA (dye:bp = 0.2:1−0.67:1). DRAQ5 changed both the DNA total length and the persistence length, while Dapi affected the persistence length. PicoGreen showed no detectable effects at low concentration. As expected at high concentrations (dye:bp > 6.7:1), we observed strong structural and topological changes in DNA when bound with dyes; with PicoGreen dye the total length of DNA increased up to 45%, without affecting the persistence length; Dapi dye decreased the persistence length by 40% but not changing the total length of DNA fragments. Interestingly DRAQ5 affected both shape parameters, increasing the total length and at the same time decreasing the persistence length.

Below we discuss how these AFM data link molecular mechanisms of each DNA−dye interaction with structural changes DNA undergoes when bound with dyes.

PicoGreen dye is assumed to intercalate into dsDNA as well as bind to minor groove,[12] though the binding mode is still not well understood. Generally screening the negative charges from the DNA backbone leads to the decrease of the persistence length.[22,23] PicoGreen carries a single positive charge; therefore, once bound to DNA, it should decrease the DNA persistence length. In our experiments the DNA persistence length was independent from the PicoGreen concentration. It can be hypothesized that the increase in the DNA flexibility due to screening of one DNA charge per bound PicoGreen molecule is somehow counteracted by the local stiffening of PicoGreen−DNA complex.[12] We measured an increase in the contour length of DNA for high PicoGreen concentrations. Intercalation leads to local unwinding and stretching of DNA in contrast to minor groove binding. On the basis of these data, we can suggest a concentration dependent PicoGreen binding. At low concentrations (PicoGreen:bp < 0.67:1) PicoGreen presumably binds

DOI: 10.1021/ma502537g
Macromolecules 2015, 48, 1860−1865

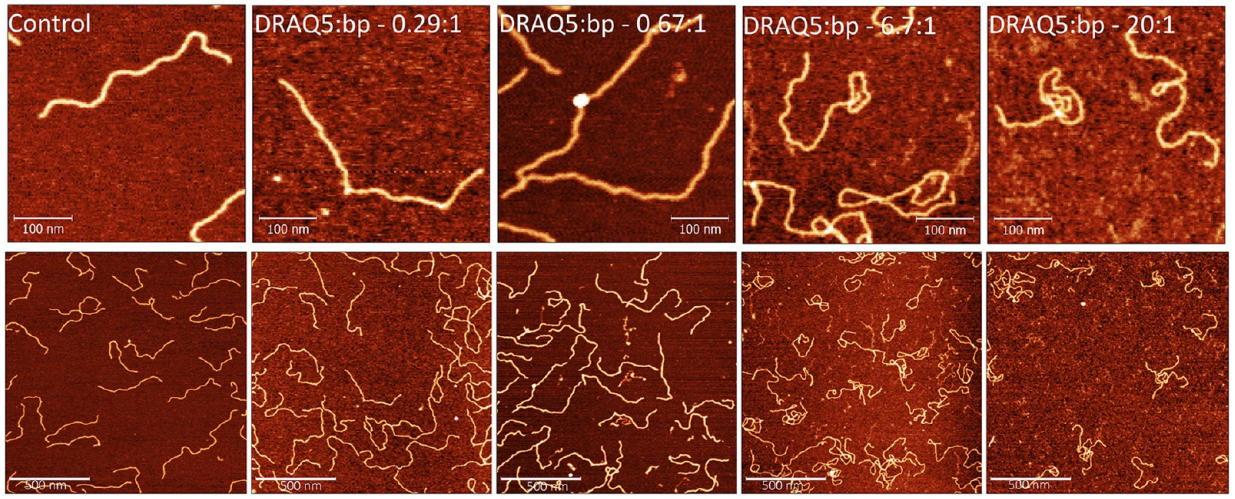

Figure 5. AFM images of control and DRAQ5 stained DNA. High concentration of DRAQ5 leads to longer and more flexible DNA structures. Scale bars for upper and lower AFM images are 100 and 500 nm, respectively.

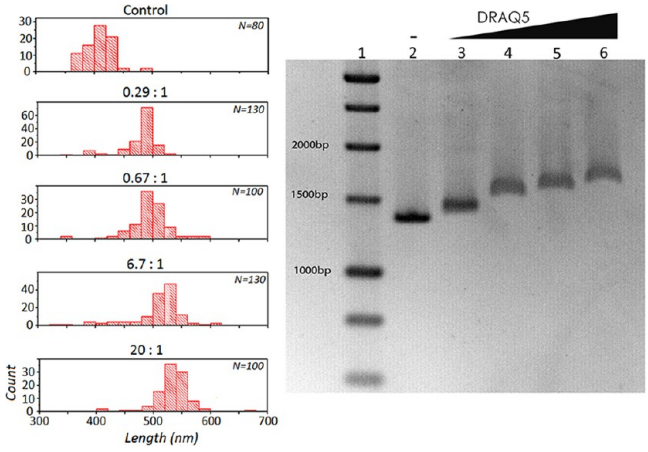

Figure 6. (A, left) Contour length distribution for DNA−DRAQ5 complexes. (B, right) The corresponding DNA gel electrophoresis image Lane 1 is the marker DNA, lane 2 control 1.4kb DNA, and lanes 3−6 show DNA stained with growing DRAQ5 concentration (DRAQ5:bp = 0.29:1; 0.67:1; 6.7:1; and 20:1).

Table 3. Shape Parameters of DNA Bound with DRAQ5 Dye

DRAQ5:bp	no. of molecules	av length	elongation [%]	L_p [nm]	ΔL_p [%]
control	80	410 ± 25		61 ± 3	
0.29:1	130	480 ± 30	16	53 ± 3	−13
0.67:1	100	495 ± 35	20	55 ± 3	−10
6.7:1	130	510 ± 45	24	44 ± 3	−28
20:1	100	535 ± 30	30	33 ± 3	−46

to DNA minor groove, and at higher concentrations (PicoGreen:bp > 6.7:1) it starts to intercalate into DNA.

DAPI dye, a minor groove binding dye, has been shown to have a preferred mode of binding to AT-rich sequences at low dye concentrations. Dapi carries a divalent positive charge; therefore, when bound to DNA minor groove it screens the negative DNA backbone charge, making it more flexible. In agreement with this model, we saw a concentration-dependent decrease in DNA persistence length. As mentioned above, minor groove binding should retain the helicity and the pitch of the dsDNA. AFM as well as the gel electrophoresis experiments confirm this notion. At low concentrations the contour length of DNA does not change (Dapi:bp < 0.67:1). Interestingly at higher concentrations it was suggested that it might change its minor groove binding mechanism and intercalate into GC-rich sequences as well.[32−35,38] At high concentrations (Dapi:bp > 6.7:1) we observe only a slight increase of the average contour length. This suggests that in our case Dapi mostly acts as a minor groove binder, even at high concentrations.

DRAQ5 is an intercalating DNA dye that has some preference to bind the minor groove in AT base-pair-rich sequences.[8,9,14,37] When bound to DNA, in contrast to PicoGreen, we observed a continuous increase in the contour length, starting from the lowest dye concentration (DRAQ5:bp = 0.29:1). These results support that DRAQ5 acts as a strong intercalator, since intercalation leads to DNA base unwinding and elongation. Surprisingly, even though the net charge of DRAQ5 is zero and it should not screen any charges from the DNA, we measured a concentration-dependent decrease in the persistence length. This behavior could be linked to the minor groove binding mode of DRAQ5 that locally decreases the DNA stiffness.[37] At low DRAQ5 concentrations we saw mostly DNA elongation (~20%) and a partial decrease in persistence length (ΔL_p ~10%). At high DRAQ5 concentrations (DRAQ5:bp > 6.7:1) the decrease in DNA persistence length become more dominant (ΔL_p ~ 45%) compared to contour length elongation (elongation ~30%). On the basis of this, we could conclude that DRAQ5 binding to DNA leads to a complex interplay of two phenomena: local unwinding due to intercalation and long-range effect of increased flexibility.

In living cells DNA exists in a form of chromatin: complex of DNA and DNA binding proteins (histones and transcription factors). The effect the dyes have on a DNA organization in living cells quantitatively can be different from naked DNA data due to the interaction between DNA and these proteins. However, there are parts of cellular DNA which are not covered by histones, particularly in active euchromatin regions. Moreover, even in chromatinized DNA there are gaps between histones where dyes can bind. In addition, minor groove binders theoretically can bind even DNA on histones. Therefore, we think that qualitatively the effect should be similar as DNA binding dyes still bind DNA.

In general, our results show that DNA binding dyes affect DNA structure depending on the binding mechanism and in a

DOI: 10.1021/ma502537g
Macromolecules 2015, 48, 1860−1865

clear concentration-dependent manner. It means that when DNA is stained possible changes in the DNA properties has to be considered.

■ ASSOCIATED CONTENT

Supporting Information

Supporting Information 1 describes how the persistence length was calculated for DNA−dye complexes; Supporting Information 2 plots the corresponding correlation functions of all DNA:dye complexes; Supporting Information 3 shows optical images of Hela cells taken after staining with different dyes. This material is available free of charge via the Internet at http://pubs.acs.org.

■ AUTHOR INFORMATION

Corresponding Author

*E-mail giovanni.dietler@epfl.ch; Ph +41 21 69 30446; Fax +41 21 693 04 22 (G.D.).

Notes

The authors declare no competing financial interest.

■ ACKNOWLEDGMENTS

Authors thank Hubert Ranchon for fruitful discussions.

■ REFERENCES

(1) Murade, C. U.; Subramaniam, V.; Otto, C.; Bennink, M. L. *Biophys. J.* **2009**, *97*, 835−843.
(2) Manneschi, C.; Angeli, E.; Ala-Nissila, T.; Repetto, L.; Firpo, G.; Valbusa, U. *Macromolecules* **2013**, *46*, 4198−4206.
(3) Yeh, J.-W.; Taloni, A.; Chen, Y.-L.; Chou, C.-F. *Nano Lett.* **2012**, *12*, 1597−1602.
(4) Keyser, U. F.; Koeleman, B. N.; van Dorp, S.; Krapf, D.; Smeets, R. M. M.; Lemay, S. G.; Dekker, N. H.; Dekker, C. *Nat. Phys.* **2006**, *2*, 473−477.
(5) Doyle, P. S.; Ladoux, B.; Viovy, J. L. *Phys. Rev. Lett.* **2010**, *84*, 4769−4772.
(6) He, Q.; Ranchon, H.; Carrivain, P.; Viero, Y.; Lacroix, J.; Blatche, C.; Daran, E.; Victor, J.-M.; Bancaud, A. *Macromolecules* **2013**, *46* (15), 6195−6202.
(7) Ashley, N.; Harris, D.; Poulton, J. *Exp. Cell Res.* **2005**, *303*, 432−446.
(8) Smith, P. J.; Wiltshire, M.; Errington, R. J. *Curr. Protoc. Cytom.* **2004**, Chapter 7, Unit 7.25.
(9) Martin, R. M.; Leonhardt, H.; Cardoso, M. C. *Cytometry, Part A* **2005**, *67*, 45−52.
(10) Benke, A.; Manley, S. *ChemBioChem* **2012**, *13*, 298−301.
(11) Günther, K.; Mertig, M.; Seidel, R. *Nucleic Acids Res.* **2010**, *38* (19), 6526−6532.
(12) Dragan, A. I.; Casas-Finet, J. R.; Bishop, E. S.; Strouse, R. J.; Schenerman, M. A.; Geddes, C. D. *Biophys. J.* **2010**, *99*, 3010−3019.
(13) Portugal, J.; Waring, M. J. *Biochim. Biophys. Acta* **1988**, *949* (2), 158−168.
(14) Wojcik, K.; Dobrucki, J. W. *Cytometry, Part A* **2008**, *73*, 555−562.
(15) Gudnason, H.; Dufva, M.; Bang, D. D.; Wolff, A. *Nucleic Acids Res.* **2007**, *35*, e127.
(16) Sischka, A.; Toensing, K.; Eckel, R.; Wilking, S. D.; Sewald, N.; Ros, R.; Anselmetti, D. *Biophys. J.* **2005**, *88*, 404−411.
(17) Bennink, M. L.; Schärer, O. D.; Kanaar, R.; Sakata-Sogawa, K.; Schins, J. M.; Kanger, J. S.; de Grooth, B. G.; Greve, J. *Cytometry* **1999**, *36* (3), 200−208.
(18) Kaji, N.; Ueda, M.; Baba, Y. *Electrophoresis* **2001**, *22*, 3357−3364.
(19) Gurrieri, S.; Wells, K. S.; Johnson, I. D.; Bustamante, C. *Anal. Biochem.* **1997**, *249*, 44−53.
(20) Ahn, S. J.; Costa, J.; Emanuel, J. R. *Nucleic Acids Res.* **1996**, *24*, 2623−2625.
(21) Nyberg, L.; Persson, F.; Akerman, B.; Westerlund, F. *Nucleic Acids Res.* **2013**, *41*, e184.
(22) Eckel, R.; Ros, R.; Ros, A.; Wilking, S. D.; Sewald, N.; Anselmetti, D. *Biophys. J.* **2003**, *85*, 1968−1973.
(23) Vladescu, I. D.; McCauley, M. J.; Nuñez, M. E.; Rouzina, I.; Williams, M. C. *Nat. Methods* **2007**, *4*, 517−522.
(24) Kleimann, C.; Sischka, A.; Spiering, A.; Tönsing, K.; Sewald, N.; Diederichsen, U.; Anselmetti, D. *Biophys. J.* **2009**, *97*, 2780−2784.
(25) Nečas, D.; Klapetek, P. *Cent. Eur. J. Phys.* **2012**, *10*, 181−188.
(26) Rubinstein, M.; Colby, R. *Polymer Physics*; Oxford University Press: Oxford, UK, 2003.
(27) Ghosh, K.; Carri, G. A.; Muthukumara, M. *J. Chem. Phys.* **2001**, *115*, 4367.
(28) Holm, C.; Joanny, J. F.; Kremer, K.; Netz, R. R.; Reineker, P.; Seidel, C.; Vilgis, T. A.; Winkler, R. G. *Adv. Polym. Sci.* **2004**, *166*, 67−111.
(29) Witz, G.; Rechendorff, K.; Adamcik, J.; Dietler, G. *Phys. Rev. Lett.* **2008**, *101*, 148103.
(30) de Gennes, P.-G. *Scaling Concepts in Polymer Physics*; Cornell University Press: Ithaca, NY, 1979.
(31) Mikhaylov, A.; Sekatskii, S. K.; Dietler, G. *J. Adv. Microsc. Res.* **2013**, Vol. *8*. N4; 241—245.
(32) Larsen, T. A.; Goodsell, D. S.; Cascio, D.; Grzeskowiak, K.; Dickerson, R. E. *J. Biomol. Struct. Dyn.* **1989**, *7*, 477−491.
(33) Kapuscinski, J. *Biotech. Histochem.* **1979**, *70* (5), 220−233.
(34) Trotta, E.; D'Ambrosio, E.; Del Grosso, N.; Ravagnan, G.; Cirillin, M.; Paci, M. *J. Biol. Chem.* **1993**, *268* (6), 3944−3951.
(35) Eriksson, S.; Kim, S. K.; Kubista, M.; Norden, B. *Biochemistry* **1993**, *32*, 2987−2998.
(36) Singer, V. L.; Jones, L. J.; Yue, S. T.; Haugland, R. P. *Anal. Biochem.* **1997**, *249*, 228−238.
(37) Njoh, K. L.; Patterson, L. H.; Zloh, M.; Wiltshire, M.; Fisher, J.; Chappell, S.; Ameer-Beg, S.; Bai, Y.; Matthews, D.; Errington, R. J.; Smith, P. J. *Cytometry, Part A* **2006**, *69A*, 805−814.
(38) Larsson, A.; Åkerman, B.; Jonsson, M. *J. Phys. Chem.* **1996**, *100*, 3252−3263.

DOI: 10.1021/ma502537g
Macromolecules 2015, 48, 1860−1865